AIP | The Journal of Chemical Physics

A new intermolecular potential for simulations of methanol: The OPLS/2016 model

D. Gonzalez-Salgado and C. Vega

Citation: The Journal of Chemical Physics **145**, 034508 (2016); doi: 10.1063/1.4958320
View online: http://dx.doi.org/10.1063/1.4958320
View Table of Contents: http://scitation.aip.org/content/aip/journal/jcp/145/3?ver=pdfcov
Published by the AIP Publishing

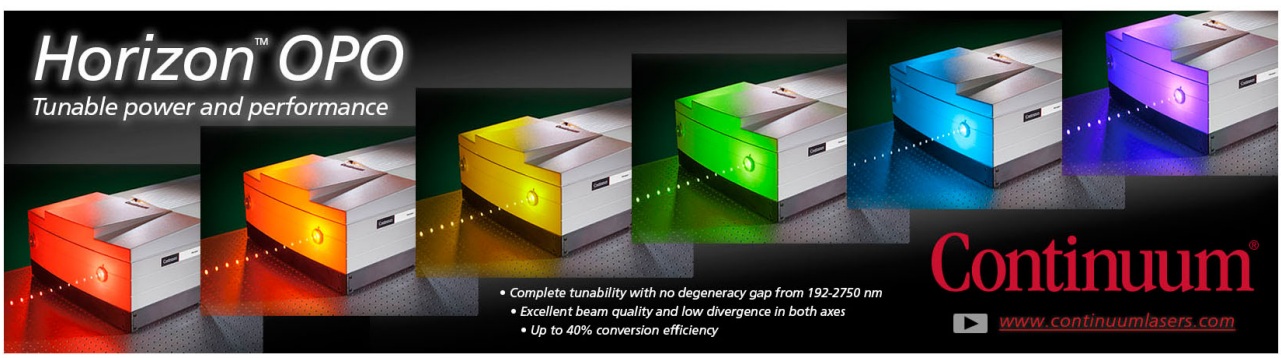

A new intermolecular potential for simulations of methanol: The OPLS/2016 model

D. Gonzalez-Salgado[1] and C. Vega[2]
[1]*Departamento de Física Aplicada, Universidad de Vigo, 32004 Ourense, Spain*
[2]*Departamento de Química Física, Facultad de Ciencias Químicas, Universidad Complutense, 28040 Madrid, Spain*

(Received 5 January 2016; accepted 27 June 2016; published online 21 July 2016)

In this work, a new rigid-nonpolarizable model of methanol is proposed. The model has three sites, located at the same positions as those used in the OPLS model previously proposed by Jorgensen [J. Phys. Chem. **90**, 1276 (1986)]. However, partial charges and the values of the Lennard-Jones parameters were modified by fitting to an adequately selected set of target properties including solid-fluid experimental data. The new model was denoted as OPLS/2016. The overall performance of this model was evaluated and compared to that obtained with other popular models of methanol using a similar test to that recently proposed for water models. In the test, a certain numerical score is given to each model. It was found that the OPLS/2016 obtained the highest score (7.4 of a maximum of 10) followed by L1 (6.6), L2 (6.4), OPLS (5.8), and H1 (3.5) models. The improvement of OPLS/2016 with respect to L1 and L2 is mainly due to an improvement in the description of fluid-solid equilibria (the melting point is only 14 K higher than the experimental value). In addition, it was found that no methanol model was able to reproduce the static dielectric constant and the isobaric heat capacity, whereas the better global performance was found for models that reproduce the vaporization enthalpy once the so-called polarization term is included. Similar conclusions were suggested previously in the analysis of water models and are confirmed here for methanol. *Published by AIP Publishing.* [http://dx.doi.org/10.1063/1.4958320]

I. INTRODUCTION

The exponential increase in computational speed over the last few decades has permitted molecular simulations of many different systems, including phenomena occurring over long time scales. A crucial aspect has been the development of simple intermolecular potentials that provide a reasonable description of the physics of the problem with low computational cost. Although different approaches have been considered, the most popular models are the site-site interaction potentials.[1] In these models, each molecule is considered as being rigid, and interaction sites are located on the positions of atoms or groups of atoms of the molecule whose coordinates are usually known from experimental studies (for instance, from X-ray or neutron diffraction). Each site typically consists of a Lennard-Jones (LJ) center and/or a partial charge. Interactions between sites are computed with the aid of the LJ potential and Coulomb's law. The determination of the parameters of the potential represents an important step when building the force field. Often the parameters of the potential are obtained to reproduce experimental properties at ambient conditions (especially the density and vaporization enthalpy). Although these potentials are often very useful, their ranges of applicability are limited and their predictions away from these conditions can be far from satisfactory. Thus, the natural evolution in the development of intermolecular potentials is to incorporate thermodynamic properties under different conditions when obtaining the parameters of the potential. A very common practice is to choose the vapour liquid equilibria (VLE) as a target property. This choice is closely related to the increasing interest in separation processes and the development of two techniques (Gibbs ensemble (GE)[2] and Gibbs-Duhem (GD) integration[3]) that allow one to determine the VLE in a rather straightforward way. In addition, one may suspect that the phase diagram contains information about intermolecular interactions. However, the phase diagram includes not only the VLE but also solid liquid equilibrium (SLE) and solid solid equilibrium (SSE) and these transitions have not been usually chosen as target properties when developing intermolecular potentials. This is surprising since the SLE and SSE have interest on their own, as also in related areas as, for instance, when studying the nucleation of the solid. Moreover, methodologies such as the Einstein Crystal (EC)[4] and the Einstein molecule (EM),[5–7] that allow one to compute chemical potentials of solid phases, are now well established and could be used when developing new force fields for simple substances.

In 2005, a general purpose model for the condensed phases of water was proposed.[8] This model, named TIP4P/2005, was elaborated using the TIP4P model of Jorgensen *et al.*[9] as starting point. The TIP4P is a four-site model with a LJ center located on the position of the oxygen atom, two partial charges on the hydrogens, and a negative charge along the bisector of the HOH angle. The parameters were obtained so as to reproduce the experimental value of the density and vaporization enthalpy at room temperature. The TIP4P/2005 model takes the geometry and

the charge distribution of the TIP4P model, but the values of the parameters were obtained to reproduce a different set of experimental properties. This set was composed of the density of liquid water under room conditions, the vaporization enthalpy at ambient temperature but corrected with the so-called polarization term, first proposed by Berendsen *et al.*,[10] the densities of several solid phases, the melting point, and several coexistence points of the SSE. A comprehensive analysis[11] of the ability of the most popular water models to describe a number of properties of water (in the gas, liquid, and solid phases) has shown that the TIP4P/2005 provides the best overall performance. The inclusion of SSE and SLE in the target properties and the implicit use of the polarization term when describing the vaporization enthalpy were found to be crucial for the overall improvement. In addition, it was found that the non-polarizable water models with the best global performance have difficulties in describing the vaporization enthalpy, the vapour pressure, the critical pressure, the dielectric constant, and the isobaric heat capacity simultaneously in both the solid and fluid phases. Any attempt to provide a reasonable description of these properties provokes the deterioration of the overall performance of the model.

All the ideas involved in the development of the TIP4P/2005 model could be used when developing intermolecular potential models for other substances. Alcohols are good candidates for this purpose due to their impact in industrial applications[12] and in basic research.[13–22] Methanol is the simplest alcohol and differs from water only in the replacement of a hydrogen atom by a methyl group. This minor difference provokes significant changes in the thermodynamic behavior. For instance, the melting point changes from 273.15 K to 175.6 K, the critical temperature from 647 K to 512.6 K, and the density at room temperature and pressure from 0.999 g cm^{-3} to 0.786 g cm^{-3}. In addition, the well known anomalies of water do not appear in methanol, its most important features being the minima of the isobaric thermal expansivity[23] and isobaric heat capacity[24–26] at very low temperatures. As for the solid state, methanol appears in four different allotropic phases,[27] α, β, γ, and δ. At atmospheric pressure, going from high to low temperatures, the fluid first crystallizes into the β form at 175.6 K. This phase is stable in a small region and it transforms at 159 K into the α phase, the stable form at low temperatures. At high pressures and very low temperatures the α phase transforms into the δ phase (a new solid phase recently discovered[27]). At high pressures and moderately low temperatures the α phase transforms into the γ phase. It is worth noting that numerous studies were performed over the α and β phase giving a reliable description of their structures and their equilibrium curves.[28–34] This is not the case for the δ and γ phases for which experimental results are rather scarce.[27,35]

The most popular intermolecular potentials used for simulations of liquid methanol are H1,[36,37] OPLS,[38] L1,[39] and L2[40,41] models. All of them are of united atom type (all atom models such as GAFF[42] or OPLS-AA[43] are not considered in this work) and have a similar geometry and site definition but different values of the parameters. For the H1 and OPLS models, the potential parameters were obtained by fitting to experimental data at ambient conditions whereas VLE data were also considered for the L1 and L2 models. In all the cases, their predictions[44,45] of the SSE and the SLE do not agree with experiments. Their melting temperatures were found to be between 35 K and 50 K higher than the experimental value. Thus, there is room for improvement.

In this work a new intermolecular potential for simulations of condensed phases of methanol is proposed. Our main aim was to find a model that provides a reasonable description of the SLE without significantly deteriorating the predictions of the VLE and the liquid phase properties. The methodology used here to obtain the new model resembles that used for the development of the TIP4P/2005 model but using, in this case, the OPLS model of Jorgensen as starting point in the optimization procedure. The second aim of this work was to analyze whether the main conclusions reached in previous works[11] about the limitations of non-polarizable intermolecular potentials of water in describing a number of properties also hold in the case of methanol.

II. THE OPTIMIZING METHOD AND THE FITTING PROPERTIES SET

The fitting procedure was based on the hypothesis that the dependence of a property Y_i on the model parameters β_j verifies the following truncated Taylor expansion:

$$Y_i \approx Y_i^0 + \sum_{j=1}^{Z}\left[\left(\frac{\partial Y_i}{\partial \beta_j}\right)\left(\beta_j-\beta_j^0\right)+\frac{1}{2}\left(\frac{\partial^2 Y_i}{\partial {\beta_j}^2}\right)\left(\beta_j-\beta_j^0\right)^2\right], \quad (1)$$

where the super-index 0 indicates values of the reference model and Z is the total number of parameters. Note that Eq. (1) is not a Taylor expansion truncated to the second order since the cross second order derivatives are not included in this equation. Estimation of the first and second order derivatives of Y_i with respect to β_j of Eq. (1) can be made on the flight[46,47] in the same simulation in which the value of Y_i^0 is obtained. We used, however, an alternative method following the next steps. First of all, the values of Y_i^0 were estimated by molecular simulation of the reference model. Secondly, the value of one parameter of the potential (say β_j) was modified (with respect to the reference model) while keeping the rest of the parameters constant and simulations were performed to evaluate Y_i. This procedure was carried out four times, using two values of β_j smaller than β_j^0 and two values larger than β_j^0. These four simulation results were then fitted to Eq. (1) to estimate the value of the first and second derivatives. This methodology was implemented for each parameter β_j and after that repeated for each target property Y_i. The objective function was defined as

$$\phi = \sum_{i=1}^{W} w_i\left(Y_i - Y_i^{exp}\right)^2, \quad (2)$$

where w_i is the weight of property i in the fit, W is the number of fitting properties, and the super-index exp refers to experimental values. The weights w_i were selected in order to give similar weight to all the properties of the fit. In the previous expression Y_i is given by Eq. (1). The values of the potential parameters of the optimized

potential $\beta_1,\beta_2,\ldots,\beta_S$ were obtained by minimizing ϕ using a Marquardt algorithm.[48]

As was stated in the Introduction, the choice of the properties to be fitted is a crucial aspect in the development of a potential model. One possible option is to select a wide variety of physical properties for each phase and at different thermodynamic states. This is not a bad solution but it has at least two shortcomings. On the one hand, the increase in the computation time for large sets of properties can make the optimization procedure impractical. On the other hand, not all the properties are equally sensitive to the intermolecular interactions and not all of them can be predicted by simple nonpolarizable intermolecular potentials. The inclusion of these types of properties in the fitting procedure can reduce the predictive ability of the model, as was shown in previous simulation studies of water.[11] Thus, we think that the best option is to consider a smaller set including the more sensitive properties to the intermolecular interactions and avoiding unpredictable magnitudes by this type of models. This philosophy was used for the construction of the TIP4P/2005 model and is used here for the definition of the OPLS/2016 model.

It is well established that the phase diagram is a signature of the intermolecular potential of the substance. Any intermolecular potential model must provide a reasonable description of the SSE, SLE, and VLE. In the case of methanol, the experimental SSE and SLE are well studied for the α and β phases[28–34] but the information concerning the γ[35] and δ[27] is incomplete. In that sense, data related with the γ and δ phases should not be selected as target properties, since only reliable experimental results must be considered. On the other hand, previous models of methanol were found to be unable to predict a clear difference between the free energies of the α and β phases due to the similarity between phases.[44,45] Therefore, only information related with the melting line must be chosen to be fitted. Particularly, we decided to include in the fitting properties set two points of the experimental melting line (fluid-β transition): the transition temperatures at 1 bar (i.e., the melting point) and at 10 000 bars. The enthalpy and volume change at melting at 1 bar were also included as a target property.

As for the VLE, a previous analysis on the predictive ability of non-polarizable water models[11] seems to indicate that forcing them to give quantitatively the vapour pressure or the vaporization enthalpy at ambient conditions results in a significant deterioration of the global performance of the model. This fact was related with the strong difference between the dipole moment of the liquid and the vapour phase, which cannot be accounted for a non-polarizable model where the dipole moment is unique. This was true for water and is also true for methanol, which has a dipole moment of 1.7 D[49] in the gas phase and of about 2.6 D[50] in the fluid phase. Despite this fact, nonpolarizable water models provide yet reasonable predictions for the orthobaric densities and the critical temperature. Results for TIP4P/2005 have indicated that a good description of the VLE can be reached by using the vaporization enthalpy at 298.15 K (including the polarization correction[10]) and the orthobaric density of the liquid at a reduced temperature (with respect to the critical temperature) of 0.8 as target properties. After realizing that the L1 model reproduces the vaporization enthalpy of methanol at room temperature quite well (when including the polarization correction) we used the potential energy of this model[45] as a target property as potential energies are computed easily. The orthobaric density of liquid methanol at 10 bar and 410 K completes the set of target properties related with the VLE.

Densities of the liquid at different temperatures and pressures were also considered as target properties. In particular densities of the liquid along the room pressure isobar at three different temperatures, namely 250 K, 298.15 K, and 323.15 K and the density at room temperature and 2000 bars were also included in the "training" set. Finally the density of the β solid phase was also included.

Therefore, all together, eleven properties ($W = 11$) were considered as target properties for the model: the melting temperature T_m at two pressures (1 bar and 1000 bars),[34] the melting enthalpy Δh_{l-s} and volume change Δv_{l-s} at 1 bar,[30] the density ρ of the β solid at 170 K,[33] the densities ρ of methanol in the fluid phase[23,51] at five different thermodynamic states (1 bar, 250 K; 1 bar, 298.15 K; 1 bar, 323.15 K; 2000 bars, 298.15 K; 10 bars, 410 K), and the potential energy U^{pot} at 298.15 K and 1 bar[45] (as given by the L1 model).

III. MODELS

The OPLS model proposed by Jorgensen[38] was used as reference model in the optimization procedure. The new model will have the same geometry as OPLS (i.e., bond distances angles and interactions sites) but with a new set of parameters ($Z = 6$) obtained after applying the optimization procedure with the 11 target properties described above. This new model will be named as methanol OPLS/2016. Properties of the new model will be compared to those of other popular models of methanol such as H1,[36,37] L1,[39] L2,[40,41] and OPLS.[38]

In all these models interaction sites are located on the methyl group, on the oxygen atom, and on the hydrogen of

TABLE I. Lennard-Jones parameters and charges of the H1, L1, L2, OPLS, and OPLS/2016 models. Values of epsilon are reported in units of the Boltzmann constant k.

Model	ϵ_{oo}/K	σ_{oo}/Å	ϵ_{cc}/K	σ_{cc}/Å	q_o/e	q_h/e	q_c/e	r_{oh}/Å	r_{oc}/Å	C–O–H
H1	87.940	3.0830	91.1500	3.8610	−0.728 00	0.431 00	0.297 00	0.9451	1.4246	108.53
L1	86.500	3.0300	105.200	3.7400	−0.700 00	0.435 00	0.265 00	0.9451	1.4246	108.53
L2	87.879	3.0300	120.592	3.7543	−0.678 74	0.431 28	0.247 46	0.9451	1.4246	108.53
OPLS	85.547	3.0700	104.166	3.7750	−0.700 00	0.435 00	0.265 00	0.9450	1.4300	108.50
OPLS/2016	97.775	3.1659	110.450	3.6499	−0.654 40	0.499 80	0.154 60	0.9450	1.4300	108.50

TABLE II. The dipole moment μ_{mod} and the principal components (Q_{xx}, Q_{yy}, Q_{zz}) of the quadrupolar tensor of the H1, L1, L2, OPLS, and OPLS/2016 models compared with experimental data and quantum mechanical calculations using Møller Plesset perturbation theory. All the QM results were taken from the NIST and their differences come from the basis set used and the level of the theory. The axis x and y are in the plane formed by the H,O and C atoms whereas the z axis is perpendicular to this plane.

Model	μ_{mod}/D	Q_{xx}/DÅ	Q_{yy}/DÅ	Q_{zz}/DÅ
H1	2.336	−1.391	−2.043	3.434
L1	2.221	−1.391	−2.060	3.451
L2	2.147	−1.376	−2.043	3.419
OPLS	2.221	−1.393	−2.065	3.458
OPLS/2016	2.178	−1.544	−2.367	3.911
Gas(exp)	1.70			
Gas(QM[a])	1.836	−1.370	−1.809	3.179
Gas(QM[b])	1.996	−1.340	−2.040	3.380
Gas(QM[c])	1.651	−1.230	−1.740	2.970
Gas(QM[d])	1.732	−1.210	−1.780	2.990

[a]MP2/6-31G*.
[b]MP2 = full/6-31+G**.
[c]MP2 = full/cc-pVTZ.
[d]B2PLYP/6-311G**.

the hydroxyl group. Partial charges and LJ centers are located on the positions of the oxygen and methyl group. For the hydrogen of the hydroxyl group, a partial charge is located on the position of the hydrogen atom (as is often done in water models). Geometries and potential parameters of all the models considered in this work are given in Table I. Dipole and quadrupole moments are given in Table II.

For all these models, the energy between sites a and b of two different molecules is given by the following expression:

$$U_{ab}^{pot} = 4\epsilon_{ab}\left[\left(\frac{\sigma_{ab}}{r_{ab}}\right)^{12} - \left(\frac{\sigma_{ab}}{r_{ab}}\right)^{6}\right] + \frac{1}{4\pi\epsilon_0}\frac{q_a q_b}{r_{ab}}, \quad (3)$$

where ϵ_{ab} and σ_{ab} are the Lennard-Jones parameters, r is the distance, and $q_{a,b}$ are the partial charges. For the models H1,L1,L2, Lorentz-Berthelot rules are used for the crossed interaction parameters, whereas for OPLS and OPLS/2016 the geometric mean was used.

IV. THE SIMULATIONS

The simulations in this work can be classified into two groups. In the first group, simulations were performed to determine the parameters of the new potential. For this purpose, a number of properties (eleven) were determined for the reference fluid (Y_i^0) and for slightly perturbed (by modifying one parameter at a time) versions (Y_i) to estimate the derivatives of Eq. (1). With these simulations the parameters of the new potential OPLS/2016 were obtained. In the second group of simulations the properties of the OPLS/2016 potential were evaluated and compared to the results of other potential models and to experimental results. In particular, the following properties were computed with the new potential: the SLE (the p–T melting line and its slope dp/dT at 1 bar, Δv_{l-s} and Δh_{l-s} at 1 bar), the VLE (the p–T line, the orthobaric densities, the critical parameters T_c, p_c, and ρ_c, and the vaporization enthalpy Δh_{v-l} at 298.15 K), the liquid densities ρ along the p = 1 bar isobar and T = 298.15 K isotherm, and finally the isobaric thermal expansivity α_p, the isothermal compressibility κ_T, the isobaric heat capacity C_p, the static dielectric constant ϵ, the surface tension γ_s, the self-diffusion coefficient D, the shear viscosity η, and the orientational relaxation time τ_2. All these properties, except for the SLE properties (determined by the authors in previous works[44,45]), were also calculated for all models considered in this work. We shall describe now how these properties were computed.

The SLE and VLE were computed using the GD integration method[3] starting from an initial coexistence point. For the SLE, the initial coexistence point (at 1 bar) was obtained by imposing the condition of equal chemical potentials between the two phases. The chemical potential of the fluid phase was obtained by using thermodynamic integration from the ideal gas state (800 K and 1 bar).[44] The chemical potential of the solid phases (α and β) was evaluated from the free energies at 100 K and 1 bar obtained using the Einstein crystal method[52] (with the Einstein molecule implementation[5–7]) followed by thermodynamic integration. To evaluate the impact of changing a parameter of the potential into the solid and fluid chemical potential, we used Hamiltonian integration.[7] The initial coexistence point for the VLE was evaluated using the direct coexistence method.[53] The solid-liquid coexistence curves were drawn through the conventional expression of the Clapeyron equation

$$\frac{dp}{dT} = \frac{\Delta h_{s-l}}{T\Delta v_{s-l}}, \quad (4)$$

where T is temperature, p is pressure, and Δh_{s-l} and Δv_{s-l} are the molar solid-liquid transition enthalpy and volume, respectively. For the estimation of the liquid-vapor curve it is usually recommended to use the Clapeyron equation modified in this way:

$$\frac{d(lnp)}{d(1/kT)} = -\frac{kT\Delta h_{l-v}}{p\Delta v_{l-v}}, \quad (5)$$

where Δh_{l-v} and Δv_{l-v} are the liquid-vapor transition enthalpy and volume, respectively. A fourth order Runge-Kutta algorithm was used to integrate both versions of the Clapeyron equation. The $p-T$ data on the VLE curve were fitted to the Antoine-type equation

$$\ln(p) = A - \frac{B}{C+T}, \quad (6)$$

where A, B, and C are fitting parameters.

The application of the GD integration method usually involves short runs which are sufficient to obtain the p–T curve but not for a precise computation of the transition enthalpy or volume. In order to get precise values for both Δh_{s-l} and Δv_{s-l} at 1 bar, the liquid and vapour densities along the binodal, ρ_l and ρ_v, and Δh_{l-v} at 298.15 K, new and longer runs are required.

The difference $(\rho_l - \rho_v)$ was fitted to the following equation in order to obtain the critical temperature T_c:

$$\rho_l - \rho_v = E\left[1 + F\left(\frac{T_c - T}{T_c}\right)^{0.5}\right]\left(\frac{T_c - T}{T_c}\right)^{0.326}, \quad (7)$$

where E, F, and T_c are fitting parameters. The critical pressure p_c was identified as the pressure given by the Antoine equation

when $T = T_c$. The critical density ρ_c was estimated by fitting $(\rho_l + \rho_v)/2$ to the following equation:

$$\frac{\rho_l + \rho_v}{2} = \rho_c + G\left(\frac{T_c - T}{T_c}\right)^{\gamma_{eff}}, \tag{8}$$

where ρ_c, G, γ_{eff} are fitting parameters.

The vaporization enthalpy Δh_{l-v} at 298.15 K was corrected by the self-polarization term proposed by Berendsen[10]

$$\Delta E_{pol} = \frac{(\mu_{mod} - \mu_v)^2}{2\alpha_{pol}}, \tag{9}$$

where α_{pol} is the polarizability. The dipole moment for each model μ_{mod} is given in Table II and $\mu_v = 1.7$ D and $\alpha_{pol} = 3.29$ Å^3 were taken from the literature.[54] The polarization term accounts for the work needed to polarize the molecule from the gas phase dipole moment to the liquid phase value.

The isobaric thermal expansivity α_p at 298 K was computed by using the incremental method[55] through the following equation:

$$\alpha_p = \frac{1}{\rho[298\text{ K}]}\left(\frac{\rho[290\text{ K}] - \rho[306\text{ K}]}{16}\right), \tag{10}$$

where the temperature to which the density is calculated is specified explicitly. The fluctuation method[56] was used for the calculation of the isothermal compressibility κ_T and the isobaric heat capacity C_p at 298.15 K.

The dielectric constant ϵ was evaluated using the well known equation[57]

$$\epsilon = 1 + \frac{4\pi}{3kTV}\langle M^2\rangle = 1 + \frac{4\pi}{3kTV}N\mu^2 G_k, \tag{11}$$

which is the correct one for simulations with Ewald summations with conducting boundary conditions. In this expression V and M denote the volume and the total dipole moment of the simulation box and the brackets denote averages along the production run. G_k is the finite system Kirkwood factor which is related to the relative orientation of the dipoles through the following equation:

$$G_k = 1 + \frac{2}{N}\sum_{i>j}^{N}\mathbf{u}_i \cdot \mathbf{u}_j, \tag{12}$$

where $\mathbf{u}_i$ denotes a unit vector in the direction of the dipole moment of the i molecule. Thus, the dielectric permittivity depends not only on the modulus of the dipole moment but also on their relative orientation. The experimental dielectric constant is a property difficult to reproduce when using nonpolarizable models with a good global performance. An explanation of this[58] has been given recently and can be summarized as follows. The determination of the parameters of a nonpolarizable model is aimed at providing a reasonable description of the potential energy surface (PES), i.e., the values of the energy (and its gradient) of the system as a function of the coordinates of the molecules. The PES is an important magnitude as it affects the Markov chain (MC) or the trajectory (MD) obtained in molecular simulations. In the case of water, the charge distribution that better mimics the PES yields a molecular dipole moment around 2.3 D. This dipole moment is higher than that of the gas phase (1.85 D) but less than that of the liquid phase (2.7 D). Notice that a reasonable PES can be obtained in spite of the bad description of the dipole moment of the molecule. The dielectric constant depends not only on PES but also on the dipole moment surface (DMS). Since the dipole moment which is good at reproducing the PES is not good at reproducing the DMS, it is not surprising that in the case of water most non-polarizable models fail in describing the dielectric constant. A correction[58] for the static dielectric constant has been proposed to take into account this deficiency (i.e., that the dipole moment that better describes the PES may not be the same as that describing the DMS),

$$\epsilon_{corr} = 1 + (\epsilon - 1)\left(\frac{\mu_l}{\mu_{mod}}\right)^2, \tag{13}$$

where μ_l is the true dipole moment of the molecule in the liquid phase and μ_{mod} is that of the model (or conversely μ_{mod} is the dipole moment of the molecule that better describes the PES and μ_l is the dipole moment that better describes the DMS in the liquid phase). Application of this correction to nonpolarizable models of water has allowed one to reproduce the experimental results. In the case of methanol, the situation is very close to that of water since the gas, liquid, and model dipole moments are 1.7 D, 2.6 D, and 2.2 D, respectively. For this reason in this work we shall analyze if including this correction improves the description of the dielectric constant of methanol.

The surface tension, γ_s, was computed using simulations having an explicit interface[59] by the mechanical route through the diagonal components P_{xx}, P_{yy}, and P_{zz} of the pressure tensor and the length of the box perpendicular to the interface L_z as follows:

$$\gamma_s = \frac{L_z}{2}\left[P_{zz} - \frac{P_{xx} + P_{yy}}{2}\right]. \tag{14}$$

The self-diffusion coefficient, D, was estimated using molecular dynamics simulations by using the Einstein equation

$$6Dt = \lim_{t\to\infty}\langle|\mathbf{r}_i(t) - \mathbf{r}_i(0)|\rangle^2, \tag{15}$$

where $\mathbf{r}_i(t)$ represents the position of the particle i at time t. The 100-1000 ps window was considered for the calculation of D.

The shear viscosity, η, is related with the auto-correlation function (ACF) of the off-diagonal components of the stress tensor $P_{\alpha\beta}$ through the Green-Kubo formula

$$\eta = \frac{V}{kT}\int_0^\infty \langle P_{\alpha\beta}(t_0)P_{\alpha\beta}(t + t_0)\rangle\, dt, \tag{16}$$

where the brackets indicate an average over different time origins (we set each simulation step as a different time origin). Since the components P_{xy}, P_{xz}, P_{yz}, $(P_{xx} - P_{yy})/2$, and $(P_{yy} - P_{zz})/2$ are mutually equivalent,[60] an average of their ACF was used as integral kernel. Convergence of this integral was obtained at times lower than 60 ps.

Reorientation dynamics[61,62] was also studied in this work. The orientational correlation time, τ_2, of the OH (covalent) bond of the methanol molecule was calculated from the

following expression:

$$\tau_2 = \int_0^\infty \langle P_2[\mathbf{e}(t) \cdot \mathbf{e}(t_0)] \rangle \, dt, \tag{17}$$

where $\mathbf{e}$ is a unit vector in the direction of the OH bond and P_2 is the second order Legendre polynomial. The role of the brackets is identical to that of Eq. (16). In this case, we store configurations each 100 ps and each of them is considered as a time origin. The integral kernel of that equation was fitted to a tri-exponential polynomial in order to perform the integral.[20]

The simulations in this work were made either with a home made Monte Carlo (MC) code or with the molecular dynamics (MD) package GROMACS (version 4.5.5).[63] We used the Monte Carlo program to determine the free energies of the solid phases (using the Einstein crystal method or Hamiltonian integration), free energies of the fluid phase, and for the Gibbs-Duhem runs. Thus, our MC program was used mostly to determine phase equilibria. Free energy calculations for the solid were performed in the NVT ensemble using the equilibrium simulation box obtained from anisotropic NpT simulations[64,65] (this is important in order to have the system under hydrostatic pressure and to remove any possible stress). Simulations for the fluid phase were performed in the isotropic NpT ensemble. In our MC runs, Ewald sums were used for electrostatic (with conducting periodical boundary conditions), and the LJ and the real space term of the Ewald sum was typically truncated at 10 Å (except for the vapor phase where the potential was truncated at about half the side of the simulation box). Long range corrections to the energy and pressure for the LJ part of the potential were included. In these MC runs, around 300 molecules were used for both the fluid and solid phases. In the Gibbs-Duhem runs, we used around 10 000 cycles (i.e., one trial move per particle and a trial volume change) for production and 10 000 cycles for equilibration. For the rest of the runs we typically used around 400 000 cycles for production.

Molecular dynamics runs with GROMACS were used to determine all properties not connected to phase equilibria (i.e., liquid densities along isobar, isotherms, α_p, κ_T, C_p, ϵ, D, η, and τ_2). We also used GROMACS to determine, via direct coexistence, simulations of the surface tension and the vapor liquid equilibria for a reference temperature that will be used as the initial temperature in the GD runs. The time step was always set to 2 fs (1 fs was preferred only for the computation of τ_2 and η) and typically the runs lasted 40 ns. Electrostatics interactions were treated with the particle mesh Ewald (PME) method[66] and conducting boundary conditions. The LJ part of the potential and the real space contribution of the Ewald contribution were truncated at around 14 Å. Long range corrections to the LJ part of the potential were included. We used typically 500 molecules in the NpT runs (864 when computing diffusion coefficients). The temperature was fixed using a Nose-Hoover thermostat[67,68] with a relaxation time of 2 ps and the pressure was fixed by using the Parrinello-Rahman barostat[65,69] with a relaxation time of 2 ps. The surface tension and the initial point of the VLE equilibria were determined from a NVT run where 2048 molecules of liquid methanol were placed in contact with vapor in an orthorhombic simulation box. In these VLE runs the cutoff radius was set to 24 Å and no Lennard-Jones long range corrections were applied.

V. RESULTS

The starting reference model for the optimizing procedure was the OPLS model. The geometry (i.e., bond angles and distances) was kept fixed and the Lennard Jones parameters and the partial charges of the new model were obtained in the optimization procedure. The intervals where the parameters were allowed to be varied were ϵ_{oo}/k (55, 125) K, σ_{oo} (2.85, 3.3) Å, ϵ_{cc}/k (74, 134) K, σ_{cc} (3.5, 4.05) Å, q_o (−0.9, −0.5) e, and q_h (0.35, 0.525) e. The parameters of the OPLS/2016 were obtained in two steps. Firstly, the optimization procedure was implemented taking the OPLS as reference to arrive at an intermediate model. Then, this intermediate model was taken as a reference (its properties and derivatives were evaluated) and then the optimization procedure was again applied to arrive at the final parameters of OPLS/2016 which are presented in Table I.

It is clear that the parameters of OPLS/2016 model differ significantly from those of the other models. In fact, these significant differences seem to indicate that the new model belongs to a different class of models than that defined by the previous ones. An important feature of the OPLS/2016 model is the close vicinity of the values of the oxygen Lennard-Jones parameters to those of the oxygen of water models (for instance, the TIP4P/2005 model of water takes the values of 93.2 K and 3.1589 Å for the epsilon and sigma LJ parameters, respectively). The oxygen charge is approximately half of that of the oxygen in water models (which seems reasonable as methanol has only a OH group and the methyl group is non-polar). The charge on the H atom is closer to the value adopted in water models but higher when compared to that of other methanol models. For the methyl group, both the partial charge and the value of σ are lower in OPLS/2016 when compared to other methanol models. On the other hand, the charge distribution of the new model provides a similar dipole moment to that of the previous models, but introduces significant differences in the quadrupole moment as can be seen in Table II. All dipole moments are within the interval (2.15-2.33) D. These values are higher than the experimental value of methanol in the gas phase (1.7 D) but lower than those found in liquid methanol (around 2.6 D) when estimated from electronic structure calculations.[50] As for the quadrupolar moment, all models present values higher than those of the molecule in the gas phase, and in the case of the OPLS/2016 model much higher. The quadrupole moment of the molecule of methanol in the liquid phase has not been estimated from *ab initio* calculations yet, so a comparison with its value in condensed matter is not possible. The higher values of the dipole and quadrupole moments of these models as compared to the gas phase were expected, and similar behavior was found in the case of water. Also, it is interesting to point out that the new model differs mostly from the previous ones in the value of the quadrupole moment rather than in the value of the dipole moment. In previous work, it has been shown that for water the quadrupole moment plays a key role when

describing both the melting point and the aspect of the phase diagram[70] and it would be interesting to check if the same applies to methanol.

The SLE of the H1, L1, L2, and the OPLS models was computed by the authors previously.[44,45] In this work, simulations of the SLE were performed only for the OPLS/2016 model and the results are reported in the supplementary material.[71] In Figure 1 and Table III, the melting line and the melting properties at 1 bar, for all the models, are compared to the experimental data. As can be seen, the OPLS/2016 model very reasonably predicts all these quantities significantly improving the predictions of the models proposed previously. It was found that models with a similar quadrupole (H1, L1, L2, and OPLS) have a similar melting point, the α phase being the stable phase at melting. The OPLS/2016 model, with a quadrupolar moment significantly different from the rest of the models, has a lower melting point with the β phase being the stable phase at melting (in agreement with the experiment). These results seem to indicate that the quadrupole must play a key role in determining the appearance of the phase diagram, as was found previously in the case of water. However, this cannot be considered as the only factor with impact on the melting properties. A more complete study is necessary to give light to this point. It should be mentioned that none of the models considered in this work were able to predict the α to β transition that occurs at high temperatures and low pressures. Either the α (H1, L1, L2, and OPLS) or the β (OPLS/2016) was found to be the stable phase at low pressures. In any case, the free energy difference between the α and β phases was found to be small and this is in agreement with experiments.

In this work, the vapor liquid equilibria of OPLS/2016 were computed. Although for some other models the VLE has been calculated in previous work,[39,72] we have decided to repeat these calculations using in all cases the same methodology in order to make a proper comparison. The direct coexistence direct method was used to estimate the vapor pressure at a selected temperature for each model. Good agreement was found between the vapor pressure of this work and the values previously reported in the literature as it is shown in Table IV. From these initial coexistence points, the

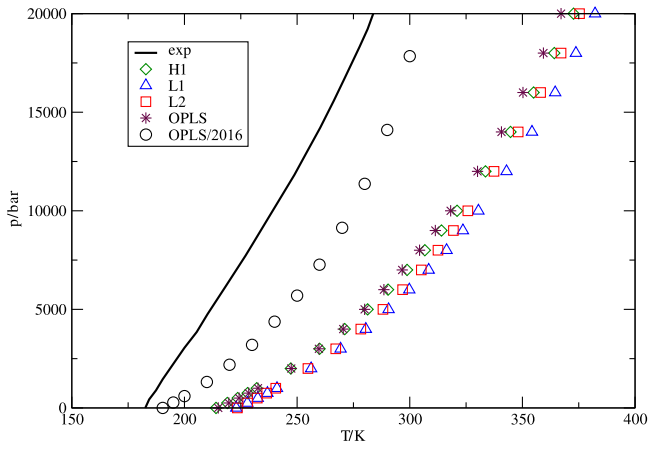

FIG. 1. Solid-fluid equilibrium of the H1, L1, L2, OPLS, and OPLS/2016 models compared to experimental results.[27]

TABLE III. Melting properties of the H1, L1, L2, OPLS and OPLS/2016 models compared to the experimental values. T_m is the melting point, dp/dT is the slope of the equilibrium curve at the melting point, Δv_{l-s} the transition volume, and Δh_{l-s} the transition enthalpy.

Model	T_m/K	(dp/dT)/bar K^{-1}	Δv_{l-s}/cm^3 mol^{-1}	Δh_{l-s}/kJ mol^{-1}
H1	214	48.0	5.05	5.19
L1	223	50.0	4.50	5.02
L2	223.5	56.0	4.24	5.31
OPLS	215	50.9	4.75	5.20
OPLS/2016	189.9	61.0	2.98	3.45
Expt.	175.6[74]	66.6	2.75[30]	3.215[30]

complete VLE was estimated using GD simulations. Liquid and vapor coexistence densities are plotted as a function of temperature in Figure 2. The L1 and L2 models were designed to provide a good description of the VLE of methanol, and this is indeed the case. The best agreement is obtained with the L2 model, whereas predictions of L1 are slightly worse, especially close to the critical point. The agreement of OPLS/2016 is similar to that of L1 although in this case, it overestimates the liquid densities at temperatures close to the critical one. The H1 model gives the poorest predictions, that of OPLS being slightly better. The critical parameters are shown in Table V. Again, the L2 model gives the best prediction of T_c. For L1 the critical temperature is slightly lower and for the OPLS/2016 slightly higher. The critical T_c of H1 and OPLS are too low. For the critical density, it is worth mentioning that the experimental values are affected by large uncertainties. We found in the literature the values of 0.269 g cm^{-3} and 0.272(2) g cm^{-3} taken from selected Refs. 73 and 74. Taking this into account, the results for the L1, L2, OPLS, and OPLS/2016 can be considered to be satisfactory and in good agreement with experiment. However, again, the H1 model shows significant deviation with respect to experiment. To finish the analysis of the VLE, the p–T curves are presented in Figure 3. In this case, the OPLS/2016(lower) and the H1(higher) give the poorest predictions whereas those of L1 and L2 model are the best ones. In summary, the OPLS/2016 model provides good predictions for orthobaric densities and for the critical density and temperature but bad results for the vapor pressure. This type of behavior was also found for the TIP4P/2005 model of water.

Before continuing, a couple of comments on the vapour pressure results are pertinent. One point concerns the bad results obtained for the vapor pressure of the OPLS/2016

TABLE IV. Vapor pressure (in bar) obtained in this work by the direct coexistence method compared to the literature values. Results for the L1, L2, and OPLS/2016 models were calculated at 450 K and those of the OPLS and the H1 model at 410 K and 390 K, respectively.

	This work	Literature
H1	9.44	
L1	25.86	25.8[39]
L2	25.80	25.2[40]
OPLS	13.19	12.86[72]
OPLS/2016	19.58	

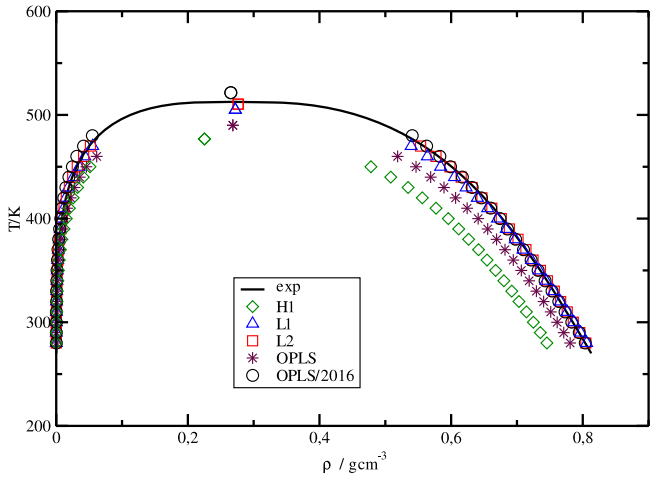

FIG. 2. Orthobaric densities plotted against temperature for all of the models considered in this work compared to experimental results.[73]

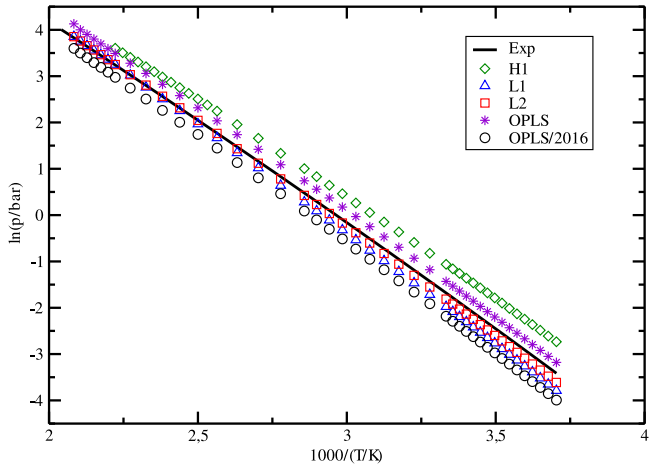

FIG. 3. Vapor-liquid equilibrium for all of the models considered in this work compared to experimental results.

which can be explained by simple thermodynamic relations. At equilibrium the chemical potentials of both the liquid and the vapour phases must be equal. By approximating the vapour as an ideal gas (which is approximately true at low temperatures), the chemical potential of the vapour takes the form $kT\ln(\rho\Lambda^3)$. In the case of the chemical potential of liquid, it reads as $(U - TS)/N$ since the term $(pV)/N$ takes nearly zero values due to the low pressures involved in the VLE at low temperatures. Taking into account that both terms must be equal, it is clear that models with lower U (this is the case of the OPLS/2016) must predict lower vapour densities and as a consequence lower vapour pressures ($p/kT = \rho$). The second aspect is the interesting behavior of the vapor pressure of the OPLS. This model reproduces the vaporization enthalpy of methanol (therefore, the value of U for this model must be reliable). However, it still yields a somewhat high vapor pressure, indicating that the chemical potential of the liquid phase is too high. This must be due to the fact that for this model (and probably for all the models of methanol considered in this work) the term -*TS* is too high for the liquid phase when compared to the experimental value. The good vapor pressure of the L2 model is probably due to a cancellation of errors between a too low value of U and a too high value of the -*TS* term. It is also interesting to point out that also in the case of water models that reproduce the vaporization enthalpy tend to overestimate the vapor pressure, thus suggesting that also for water the -*TS* term of the liquid phase is too high.

TABLE V. Critical temperature T_c, critical pressure p_c, and critical density ρ_c for the H1, L1, L2, OPLS, and OPLS/2016 compared to the experimental values.

Model	T_c/K	p_c/bar	ρ_c/g cm^{-3}
H1	476.8	61	0.225
L1	505.0	77	0.269
L2	510.4	80	0.273
OPLS	490.0	70	0.265
OPLS/2016	521.5	75	0.272
Expt.	512.6[73]	81[73]	0.272[74]/0.269[73]

The density of liquid methanol as a function of temperature and pressure for all models is plotted in Figures 4 and 5 along with the experimental results. In both cases, the worst results are those of H1 and OPLS models, whereas those of L1, L2, and OPLS/2016 models are good and similar. In more detail, one can observe that L2 gives a better prediction of the behavior with temperature than that of the L1 and OPLS/2016. The opposite appears in the dependence with pressure of the density where L1 and OPLS/2016 provide the best description. As can be seen the OPLS/2016 gives a reasonable description of the EOS of methanol with similar performance to that of the L1 and L2 models.

In Table VI a comparison of a variety of physical properties at 298.15 K and 1 bar for all the models with the experimental counterpart is presented. As for the volumetric properties, the best global performance is provided by the OPLS/2016 followed by L1 and L2 models, the results for H1 being the worst. In more detail, OPLS/2016, L1, and L2 give very good predictions for the density and differences appear for the isothermal compressibility and the isobaric thermal expansivity. The OPLS/2016 (L2) accurately predicts κ_T (α_p) and slight (strong) deviations were found for $\alpha_p(\kappa_T)$. The L1

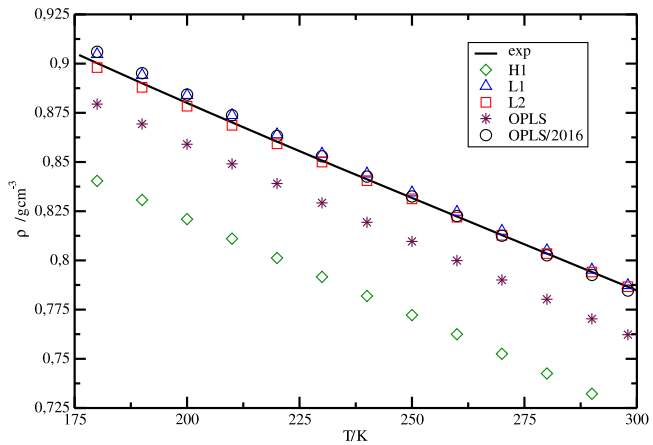

FIG. 4. Densities (at p = 1 bar) plotted against temperature for all of the models considered in this work compared to experimental results.

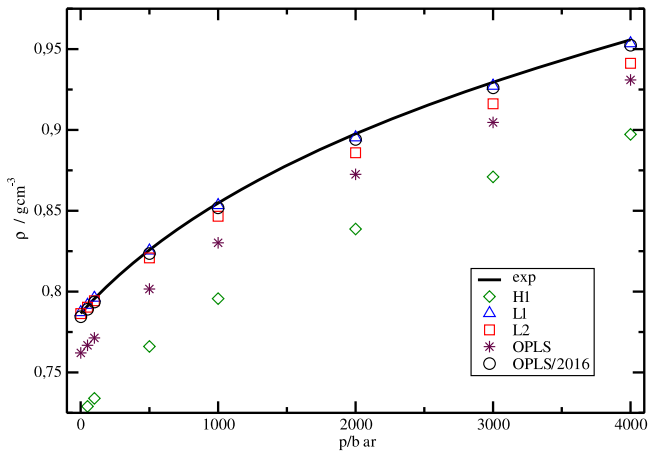

FIG. 5. Densities plotted against pressure for all of the models considered in this work compared to experimental results.

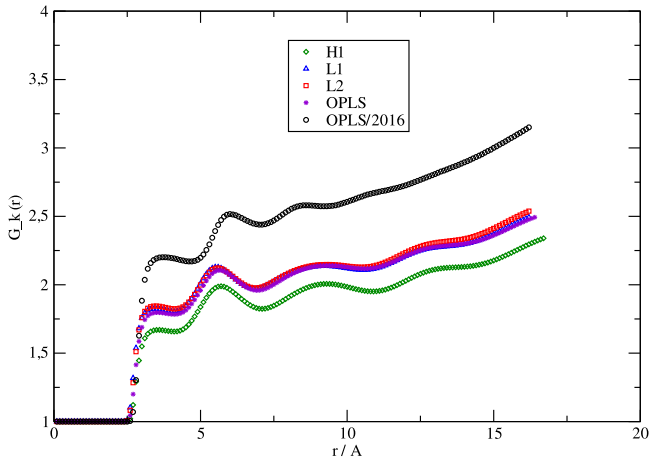

FIG. 6. Dependence of the G_k Kirkwood factor with the radius r centered in one dipole.

model deviates slightly for both properties. As for the isobaric heat capacity, all the models deviate by around 4 J mol^{-1} K^{-1} except the H1 (8 J mol^{-1} K^{-1}). This apparent good agreement is however fictitious as can be understood if we decompose this quantity into an ideal gas term and a residual contribution. The ideal gas contribution to the isobaric heat capacity takes the value 4R (33.25 J mol^{-1} K^{-1}) in computer simulations (for rigid models 3/2R from translation and 3/2R from rotation and R from the pV term). However, the experimental value of the ideal isobaric heat capacity (which includes contributions from internal roto-vibrational degrees of freedom) adopts the value[75] of 45 J mol^{-1} K^{-1}. Thus, when comparing the residual isobaric heat capacities, the comparison is not so good: 36 J mol^{-1} K^{-1} in experiments and about 53 J mol^{-1} K^{-1} in simulations. The discrepancy is most likely due to contribution of nuclear quantum effects to the heat capacity in systems with hydrogen bonds. In fact, in the case of water, it has been shown that most of the models overestimate the experimental value of C_p and the agreement with experiment improves significantly when nuclear quantum effects are included.[76] We have also computed the value of the residual contribution to C_p in solid phases (see the discussion below), and again found that simulations significantly overestimate the experimental values. The conclusion is that the heat capacity is a property that is not well reproduced when performing classical simulations of rigid non-polarizable models.

The next property to be analyzed is the static dielectric constant. Results for the dielectric constant are presented in Table VI compared to the experimental value.[77] As can be seen, all models significantly underestimate the dielectric constant. The value of the OPLS/2016 model is however a bit higher than that of the rest of the models. In order to analyze the origin of this difference, we decompose the last term of Eq. (11) into a product of two terms, $4\pi N\mu^2/3kTV$ and G_k. The values obtained for the H1, L1, L2, OPLS, and OPLS/2016 are (7.57, 2.71), (7.44, 2.93), (6.95, 2.91), (7.20, 2.86), and (7.13, 3.56), respectively. It is clear that the main difference between the OPLS/2016 and the rest of the models resides in the value of G_k which is related to the relative orientation of the dipoles. This can be also seen in Fig. 6 where the G_k factor is plotted as a function of the distance between dipoles; $G_k(r)$ is computed through Eq. (12) by considering only dipoles separated by distances between oxygens lower than r. This property shows the distance dependence of dipolar correlations in a liquid. As can be seen,

TABLE VI. Comparison of the values of several properties of methanol predicted by the H1, L1, L2, OPLS, and OPLS/2016 models at 298.15 K with the experimental counterpart. ρ denotes density, α_P isobaric thermal expansivity, κ_T isothermal compressibility, C_p isobaric heat capacity, ϵ dielectric constant, Δh_{v-l} vaporization enthalpy, and γ_s surface tension. The values in parenthesis include the scaling correction to the dielectric constant, and the polarization correction to the vaporization enthalpy.

Model	ρ g cm^{-3}	α_P kK^{-1}	κ_T T Pa^{-1}	C_p J mol^{-1} K^{-1}	ϵ	Δh_{v-l} kJ mol^{-1}	γ_s mJ m^{-2}
H1	0.724	1.45	1511	89	21.5 (25.5)	35.71 (32.00)	20.1
L1	0.787	1.26	1202	84	22.8 (29.9)	39.69 (37.20)	24.2
L2	0.787	1.21	1062	86	21.2 (29.6)	39.13 (37.30)	26.9
OPLS	0.762	1.33	1302	86	21.6 (28.3)	37.40 (34.91)	22.7
OPLS/2016	0.785	1.28	1236	86	26.4 (36.1)	39.65 (37.55)	24.7
Expt.	0.786[23]	1.20[23]	1248[51]	81.5[24]	32.7[77]	37.43[74]	22.51[78]

TABLE VII. Self-diffusion coefficient D, shear viscosity η, and orientational correlation time τ_2 at 260 K and 298 K for all the models of this work compared with experimental data.

	$10^5 D$/cm^2 s^{-1}	η/mPa s	τ_2/ps
Model	260 K–298 K	260 K–298 K	260 K–298 K
H1	1.25–3.01	0.81–0.39	6.90–2.94
L1	0.80–2.01	1.25–0.59	10.48–4.29
L2	0.90–2.21	1.11–0.56	9.49–3.87
OPLS	1.13–2.64	0.91–0.43	7.77–3.30
OPLS/2016	1.14–2.72	0.95–0.46	8.81–3.46
Expt.	1.18–2.44[79]	1.00–0.54[80]	9.06–4.73[81]

TABLE VIII. Experimental and simulation data for all the methanol models and all the chosen properties for the test. Neither the scaling correction (dielectric constant) nor the polarization correction (vaporization enthalpy) were included when reporting the results of a certain model.

Property	Expt.	H1	L1	L2	OPLS	OPLS/2016	Tol (%)
Enthalpy of phase change (kJ mol^{-1})							
Δh_{l-s}	3.215	5.19	5.02	5.31	5.2	3.45	5
Δh_{v-l} [298 K]	37.43	35.71	39.69	39.13	37.4	39.65	2.5
Critical point properties							
T_c /K	512.6	476.8	505.0	510.4	490.0	521.5	2.5
ρ_c /g cm^{-3}	0.272	0.225	0.269	0.273	0.265	0.272	2.5
p_c /bar	81	61	77	80	70	75	5
Surface tension (mN/m)							
γ_s [298 K]	22.51	20.1	24.2	26.9	22.7	24.7	2.5
Melting properties							
T_m /K	175.6	214	223	223.5	215	189.9	2.5
Δv_{l-s} /cm^3 mol^{-1}	2.750	5.050	4.500	4.240	4.750	2.98	2.5
dp/dT /bar K^{-1}	66.6	48	50	56	50.9	61.0	5
EOS 1 bar isobar (g cm^{-3})							
ρ [298 K;1 bar]	0.786	0.724	0.787	0.787	0.762	0.785	0.5
ρ [250 K;1 bar]	0.832	0.772	0.834	0.831	0.810	0.833	0.5
ρ [200 K;1 bar]	0.880	0.821	0.884	0.878	0.859	0.884	0.5
Isothermal compressibility (T Pa^{-1})							
κ_T [1 bar; 298 K]	1248	1511	1202	1062	1302	1236	5
Vapour pressure (bar)							
p_v [350 K]	1.613	2.73	1.32	1.53	2.10	1.09	5
p_v [450 K]	25.55	36.68	25.86	25.80	32.78	19.58	5
Isobaric heat capacity (J mol^{-1} K^{-1})							
C_p [liq 298 K; 1 bar]	81.5	89.0	84	86	86	86	5
C_p^{res} [liq 298 K; 1 bar]	37.4	56.0	51	53	53	53	5
C_p^{res} [α 150 K; 1 bar]	18.8	22.0	26	27	26	29	5
C_p^{res} [β 170 K; 1 bar]	10.9	31.0	33	33	33	32	5
Static dielectric constant							
ϵ [298 K]	32.7	21.5	22.8	21.2	21.6	26.4	5
Isobaric thermal expansivity (kK^{-1})							
α_p [298 K;1 bar]	1.200	1.450	1.260	1.210	1.330	1.280	5
Densities of solids (g cm^{-3})							
ρ_α [160 K;1 bar]	1.015	0.955	1.022	1.006	0.994	0.987	0.5
ρ_β [170 K;1 bar]	0.992	0.953	1.019	1.003	0.991	0.988	0.5
ρ_γ [298 K;40 000 bars]	1.353	1.235	1.304	1.277	1.276	1.291	0.5
EOS high pressure (g cm^{-3})							
ρ [298 K;5000 bars]	0.826	0.766	0.825	0.821	0.802	0.823	0.5
ρ [298 K;20 000 bars]	0.897	0.839	0.895	0.886	0.873	0.894	0.5
Self-diffusion coefficient (10^5 cm^2/s)							
D [298 K;1 bar]	2.44	3.01	2.01	2.21	2.64	2.72	5.0
D [260 K;1 bar]	1.18	1.25	0.80	0.90	1.13	1.14	5.0
Shear viscosity (mPa s)							
η [298 K;1 bar]	0.54	0.39	0.59	0.56	0.43	0.46	5.0
η [260 K;1 bar]	1.00	0.81	1.25	1.11	0.91	0.95	5.0
Orientational relaxation time (ps)							
τ_2 [298 K;1 bar]	4.73	2.94	4.29	3.87	3.3	3.46	5.0
τ_2 [260 K;1 bar]	9.06	6.90	10.48	9.49	7.77	8.81	5.0

L1, L2, and OPLS have almost equal curves, H1 is similar but with slightly lower values, whereas OPLS/2016 differ from the others not only in the values but also in the position of the maxima. When the static dielectric constant values are corrected (with the scaling correction previously described that uses the dipole moment of the molecule in the liquid phase), the results are much better. With this correction, the deviation from experiment for models L1, L2 and OPLS/2016 is about 10%.

Concerning the vaporization enthalpy, one can see from the results of Table VI that the estimate of the H1 model is low, OPLS provides an excellent prediction and those of L1, L2 and OPLS/2016 are too high. If one includes the self-polarization correction, then the predictions of L1, L2 and OPLS/2016 are quite reasonable. Establishing similarities with water, one could state that the behavior of OPLS resembles that of TIP4P in water, and the models L1, L2, and OPLS/2016 (which reproduce the behavior of the vaporization enthalpy of methanol only when including the polarization correction) behave in a similar way to models like SPC/E or TIP4P/2005 in water. Discussion of Table VI finishes with the analysis of the results of the surface tension. All models (but H1) overestimate the experimental value,[78] the predictions of OPLS being the best. Finally, the dynamics of the OPLS/2016 model was analysed using the self-diffusion coefficient D, the shear viscosity η, and the orientational correlation time τ_2. Values of these quantities for the OPLS/2016 model are compared in Table VII to those of the rest of the models and to experimental data.[79–81] As it can be seen, the OPLS/2016 model provides an accurate description of all these quantities at 260 K but its predictions are a bit worse at 298 K.

We shall now evaluate the overall performance of the five models of methanol considered in this work. We admit that there is no unique way of doing this global evaluation. We shall use here the same procedure that was used recently to evaluate the performance of water models[11] and that was adapted for DFT calculations.[82] We hope that this may be a useful way to introduce some discussion about current limits of non-polarizable models for methanol. The score will also allow to identify progress in the modeling of methanol when it comes, as it allowed to identify progress in the modeling of water.[47] First of all, it is necessary to make a selection of methanol properties. The complete list of selected properties includes the enthalpies of phase change, critical point properties, surface tension, melting properties, EOS in the 1 bar isobar and in the 298 K isotherm, isothermal compressibility, isobaric heat capacity, isobaric thermal expansivity, vapour pressure, densities of the solids, dielectric constant, self-diffusion coefficient, shear viscosity, and orientational correlation times. The selected properties were taken from different thermodynamic conditions and from different phases (gas, liquid, and solid). The second step requires one to provide a numerical score to the prediction of a model for certain property X by comparing this prediction to its experimental counterpart X_{exp}. This was made through the following expression:

$$\xi = min\left\{anint\left[10 - abs\left(\frac{(X - X_{exp}) \times 100}{X_{exp} \times tol}\right)\right], 0\right\}, \qquad (18)$$

where *min* is the minimum function, *anint* the nearest integer function, and the tolerance *tol* is given as a percentage.

This equation works as follows. The essential quantity to be computed is the relative deviation of the estimation of a property for a model. If this quantity is within 0.5 times the tolerance the score is ten points. If the deviation is between 0.5 and 1.5 times the tolerance, the score is nine points, and so on. Zero points are assigned when the deviation is ten times the tolerance. The tolerance in a specific property must be set in order to take into account the uncertainty of both the

TABLE IX. Scores.

Property	H1	L1	L2	OPLS	OPLS/2016
Enthalpy of phase change					
Δh_{l-s}	0	0	0	0	9
Δh_{v-l} [298 K]	8	8	8	10	8
Critical point properties					
T_c	7	9	10	8	9
ρ_c	3	10	10	9	10
p_c	5	9	10	7	9
Surface tension					
γ_s [298 K]	6	7	2	10	6
Melting properties					
T_m	1	0	0	1	7
Δv_{l-s}	0	0	0	0	7
dp/dT	4	5	7	5	8
EOS 1 bar isobar					
ρ [298 K;1 bar]	0	10	10	4	10
ρ [250 K;1 bar]	0	9	10	5	10
ρ [200 K;1 bar]	0	9	10	5	9
Isothermal compressibility					
κ_T [1 bar; 298 K]	6	9	7	9	10
Vapour pressure					
p_v [350 K]	0	6	9	4	4
p_v [450 K]	1	10	10	4	5
Isobaric heat capacity					
C_p [liq 298 K; 1 bar]	8	9	9	9	9
C_p^{res} [liq 298 K; 1 bar]	0	3	2	2	2
C_p^{res} [α 150 K; 1 bar]	7	2	1	2	0
C_p^{res} [β 170 K; 1 bar]	0	0	0	0	0
Static dielectric constant					
ϵ [298 K]	3	4	3	3	6
Isobaric thermal expansivity					
α_p [298 K;1 bar]	6	9	10	8	9
Densities of solids					
ρ_α [160 K;1 bar]	0	9	8	6	5
ρ_β [170 K;1 bar]	2	5	8	10	9
ρ_γ [298 K;40 000 bars]	0	3	0	0	1
EOS high pressure					
ρ [298 K;5000 bars]	0	10	9	4	9
ρ [298 K;20 000 bars]	0	10	7	4	9
Self-diffusion coefficient					
D [298 K;1 bar]	5	6	8	8	8
D [260 K;1 bar]	9	4	5	9	9
Shear viscosity					
η [298 K;1 bar]	4	8	9	6	7
η [260 K;1 bar]	6	5	8	8	9
Orientational relaxation time					
τ_2 [298 K;1 bar]	2	8	6	4	5
τ_2 [260 K;1 bar]	5	7	9	7	9

experimental and the simulation results and the importance assigned to an accurate prediction of that property in the final scoring. We set the same values that were chosen for the evaluation of water models (we refer to that paper[11] for a detailed explanation of the selection of tolerances) despite that for some properties the uncertainty of the experimental results is different. This selection, however, will allow us to compare the global performance of methanol models with that of water. Readers can, however, modify the tolerances by using the worksheet provided as supplementary material.[71]

Table VIII shows the complete list of selected properties with the experimental values and the predictions for all the models considered in this work as well as the selected tolerance. All results in Table VIII were obtained in this work except those of the SLE of the literature models that were taken from our previous works.[44,45] We have already presented and discussed most of the results of Table VIII. The only exceptions are the densities and isobaric heat capacities of the solid phases of methanol that are now included in Table VIII. The score obtained for each property and model is presented in Table IX whereas that of the final score is presented in Table X.

As can be seen, the OPLS/2016 obtained the highest score (7.4 of a maximum of 10) followed by L1 (6.6), L2 (6.4), OPLS (5.8), and H1 (3.5) models. The OPLS/2016 improves the overall description of methanol by improving the description of SLE, without deteriorating the rest of the properties. In fact if the SLE equilibrium properties were removed from the test, then the overall performance of OPLS/2016 would be quite similar to that of L1 and L2 models. One must realize that the model with the highest score does not provide the best performance for all the properties selected. If someone is interested, for instance, in the surface tension, it is more advisable to use the model with the highest score for this property (in this case the OPLS model). We strongly recommend to use the OPLS/2016 model in the region of low temperatures, when studying solid phases, or in future studies dealing with the nucleation of the solid from the supercooled liquid.

TABLE X. Scoring summary.

Scoring summary	H1	L1	L2	OPLS	OPLS/2016
Enthalpy of phase change	4.0	4.0	4.0	5.0	8.5
Critical point properties	5.0	9.3	10.0	8.0	9.3
Surface tension	6.0	7.0	2.0	10.0	6.0
Melting properties	1.7	1.7	2.3	2.0	7.3
EOS 1 bar isobar	0.0	9.3	10.0	4.7	9.7
Isothermal compressibility	6.0	9.0	7.0	9.0	10.0
Vapour pressure	0.5	8.0	9.5	4.0	4.5
Isobaric heat capacity	3.8	3.5	3.0	3.3	2.8
Static dielectric constant	3.0	4.0	3.0	3.0	6.0
Isobaric thermal expansivity	6.0	9.0	10.0	8.0	9.0
Densities of solids	0.7	5.7	5.3	5.3	5.0
EOS high pressure	0.0	10.0	8.0	4.0	9.0
Self-diffusion coefficient	7.0	5.0	6.5	8.5	8.5
Shear viscosity	5.0	6.5	8.5	7.0	8.0
Orientational relaxation time	3.5	7.5	7.5	5.5	7.0
Final score	3.5	6.6	6.4	5.8	7.4

One of the aims of this work was to propose a model that improves the description of the solid properties and of the SLE and that provides an overall good description of the properties of methanol. In view of the results of Table X we believed we achieved our initial goal.

VI. CONCLUSIONS

In this work we developed a new force field for methanol while maintaining the OPLS geometry. In addition to a number of properties from the liquid phase, properties from the solid phases and SLE were also included in the list of target properties to be reproduced by the potential. The procedure used resembles that used previously to build the TIP4P/2005 model of water starting from the TIP4P model. The new model was denoted as OPLS/2016 and a number of properties were determined for this model. The predictions of the new model were compared to those of other popular models of methanol and to the experimental results. A quantitative description of the performance of the new model was provided after performing a similar test to that used previously for water.

- The OPLS/2016 is a reasonable model of methanol. However, it is not able to reproduce all properties of methanol.
- The maximum score in the evaluation test applied to the non-polarizable united atom models of methanol of this work was located at 7.4. This is similar to the score obtained by the TIP4P/2005 model of water. It is, however, not clear if this is the maximum score that you can obtain with a rigid non-polarizable model since the complete parameter space (including bond angle and distances) was not explored.
- Models with a good overall score (i.e., L1, L2, and OPLS/2016) do not reproduce the vaporization enthalpy. In fact they overestimate the vaporization enthalpy and only reproduce the experimental value when one includes the polarization correction. Thus, it seems that models that use the polarization correction to reproduce the vaporization enthalpy yield an overall better performance than those models that reproduce the vaporization enthalpy without the polarization correction (as, for instance, OPLS). This point was also observed for water nonpolarizable models. OPLS/2016 improves the score of L1 and L2 by about 0.8 points, the improvement coming mainly from the prediction of SLE properties. Without including these properties in the evaluation test, OPLS/2016 provides a score similar to that of L1 and L2.
- Heat capacities are too high and dielectric constants are too low for the models of methanol considered in this work. In the case of water, no non-polarizable model was able to give a reasonable description simultaneously of these properties in both liquid and solid phase. It seems that these two properties are difficult to be described when using non-polarizable models. In any case, a more complete analysis including the variation of the geometry of the molecules

must be done in order to clarify this point. The low value of the dielectric constant of methanol for most of the models can be explained (and corrected) by taking into account that the dipole moment of these models (i.e., around 2.2 D) is good for describing the PES, but it is not good for describing the DMS since the true dipole moment of methanol in condensed matter seems to be closer to a value of 2.6 D.

- The melting point and aspect of the phase diagram of methanol seems to be related to the value of the quadrupole moment of the model (as was found for water in previous work). In any case, the complete set of factors that have some influence in the melting properties remains yet unknown.
- When comparing OPLS to OPLS/2016 the overall score improves by 1.6 points. Thus including SLE in the set of target properties and using the polarization correction when describing the vaporization enthalpy seems to improve the overall description of methanol when using a rigid non-polarizable model.
- It is likely that including polarization in methanol (with a well designed model) will significantly improve the overall score in the test. The challenge now is to propose a polarizable united atom model of methanol which obtains a score higher than 7.4. This model is not yet available. Including flexibility may also help, but perhaps less than the inclusion of polarization. At least this was true for water and it is likely that the same will occur for methanol.
- The new model OPLS/2016 will be very useful for future studies dealing with the nucleation of the solid phases of methanol where a description of melting temperature, coexistence densities, and melting enthalpy is needed. Those studies[83,84] typically require hundred of thousands of molecules and for this reason, a computationally cheap while still reasonable model (such as OPLS/2016) is needed.

ACKNOWLEDGMENTS

C.V. would like to thank Project Nos. FIS2013-42309P and UCM/Santander 910570 for funding. D.G.S. wants to thank Project No. FIS2011-29614 for financial support and CESGA for the use of its computation facilities. We want to thank Dr. Carl McBride for a critical reading of the manuscript.

[1]M. P. Allen and D. J. Tildesley, *Computer Simulation of Liquids* (Oxford University Press, 1987).
[2]A. Z. Panagiotopoulos, Mol. Phys. **61**, 813 (1987).
[3]D. A. Kofke, J. Chem. Phys. **98**, 4149 (1993).
[4]D. Frenkel and A. J. C. Ladd, J. Chem. Phys. **81**, 3188 (1984).
[5]C. Vega and E. G. Noya, J. Chem. Phys. **127**, 154113 (2007).
[6]E. G. Noya, M. M. Conde, and C. Vega, J. Chem. Phys. **129**, 104704 (2008).
[7]C. Vega, E. Sanz, J. L. F. Abascal, and E. G. Noya, J. Phys.: Condens. Matter **20**, 153101 (2008).
[8]J. L. F. Abascal and C. Vega, J. Chem. Phys. **123**, 234505 (2005).
[9]W. L. Jorgensen, J. Chandrasekhar, J. D. Madura, R. W. Impey, and M. L. Klein, J. Chem. Phys. **79**, 926 (1983).
[10]H. J. C. Berendsen, J. R. Grigera, and T. P. Straatsma, J. Phys. Chem. **91**, 6269 (1987).
[11]C. Vega and J. L. F. Abascal, Phys. Chem. Chem. Phys. **13**, 19663 (2011).
[12]E. D. Sloan, Nature **426**, 353 (2003).
[13]C. A. Cerdeirina, D. Gonzalez-Salgado, L. Romani, M. C. Delgado, L. A. Torres, and M. Costas, J. Chem. Phys. **120**, 6648 (2004).
[14]C. A. Cerdeirina, J. Troncoso, D. Gonzalez-Salgado, G. Garcia-Miaja, G. O. Hernandez-Segura, D. Bessieres, M. Medeiros, L. Romani, and M. Costas, J. Phys. Chem. B **111**, 1119 (2007).
[15]J. Peleteiro, J. Troncoso, D. Gonzalez-Salgado, J. L. Valencia, M. Souto-Caride, and L. Romani, J. Chem. Thermodyn. **37**, 935 (2005).
[16]D. Gonzalez-Salgado, J. Troncoso, F. Plantier, J. L. Daridon, and D. Bessieres, J. Chem. Thermodyn. **38**, 893 (2006).
[17]J. Peleteiro, J. Troncoso, D. Gonzalez-Salgado, J. L. Valencia, C. A. Cerdeirina, and L. Romani, Int. J. Thermophys. **25**, 787 (2004).
[18]C. A. Cerdeirina, C. A. Tovar, D. Gonzalez, E. Carballo, and L. Romani, Fluid Phase Equilib. **179**, 101 (2001).
[19]A. Vrhovsek, O. Gereben, A. Jamnik, and L. Putsztai, J. Phys. Chem. B **115**, 13473 (2011).
[20]A. A. Vartia, K. R. Mitchell-Koch, G. Stirnemann, D. Laage, and W. H. Thompson, J. Phys. Chem. B **115**, 12173 (2011).
[21]J. L. Kern, T. J. Flynn, Z. Wang, W. H. Thomson, and B. B. Laird, Fluid Phase Equilib. **411**, 81 (2016).
[22]B. Chen, J. J. Potoff, and J. I. Siepmann, J. Phys. Chem. B **105**, 3093 (2001).
[23]I. Cibulka, Fluid Phase Equilib. **89**, 1 (1994).
[24]M. Zabransky, V. Ruzicka, V. Majer, and E. S. Domalski, *Heat Capacity of Liquids. Critical Review and Recommended Values* (American Chemical Society, Washington, DC, 1996).
[25]M. Zabransky, V. Ruzicka, and V. Majer, J. Phys. Chem. Ref. Data **19**, 719 (1990).
[26]M. Zabransky, V. Ruzicka, and E. S. Domalski, J. Phys. Chem. Ref. Data **30**, 1199 (2001).
[27]M. V. Kondrin, A. A. Pronin, Y. B. Lebed, and V. V. Brazhkin, J. Chem. Phys. **139**, 084510 (2013).
[28]G. S. Parks, J. Am. Chem. Soc. **47**, 338 (1925).
[29]K. K. Kelley, J. Am. Chem. Soc. **51**, 180 (1929).
[30]L. A. K. Staveley and M. A. P. Hogg, J. Chem. Soc. **1954**, 1013.
[31]B. J. Tauer and W. N. Lipscomb, Acta Cryst. **5**, 606 (1952).
[32]B. H. Torrie, S.-X. Weng, and B. M. Powell, Mol. Phys. **67**, 575 (1989).
[33]B. H. Torrie, O. S. Binbrek, M. Strauss, and I. P. Swainson, J. Solid State Chem. **166**, 415 (2002).
[34]E. L. Gromnitskaya, O. V. Stal'gorova, O. F. Yagafarov, V. V. Brazhkin, A. G. Lyapin, and S. V. Popova, JETP Lett. **80**, 597 (2004).
[35]D. R. Allan, S. J. Clark, M. J. P. Brugmans, G. J. Ackland, and W. L. Vos, Phys. Rev. B **58**, R11809 (1998).
[36]M. Haughney, M. Ferrario, and I. R. McDonald, Mol. Phys. **58**, 849 (1986).
[37]M. Haughney, M. Ferrario, and I. R. McDonald, J. Phys. Chem. **91**, 4934 (1987).
[38]W. L. Jorgensen, J. Phys. Chem. **90**, 1276 (1986).
[39]M. E. van Leeuwen and B. Smit, J. Phys. Chem. **99**, 1831 (1995).
[40]T. Schnabel, A. Srivastava, J. Vrabec, and H. Hasse, J. Phys. Chem. B **111**, 9871 (2007).
[41]G. Guevara-Carrion, C. Nieto-Draghi, J. Vrabec, and H. Hasse, J. Phys. Chem. B **112**, 16664 (2008).
[42]J. Wand, R. M. Wolf, J. W. Caldwell, P. A. Kollman, and D. A. Case, J. Comput. Chem. **25**, 1157 (2004).
[43]W. L. Jorgensen, D. S. Maxwell, and J. Tirado-Rives, J. Am. Chem. Soc. **118**, 11225 (1996).
[44]D. G. Salgado and C. Vega, J. Chem. Phys. **132**, 094505 (2010).
[45]D. Gonzalez-Salgado, A. Dopazo-Paz, P. Gomez-Alvarez, J. M. Miguez, and C. Vega, J. Phys. Chem. B **115**, 3522 (2011).
[46]L. P. Wang, T. J. Martinez, and V. S. Pande, J. Phys. Chem. Lett. **5**, 1885 (2014).
[47]L.-P. Wang, T. Head-Gordon, J. W. Powder, P. Reng, J. D. Chodera, P. K. Eastman, T. J. Martinez, and V. S. Pande, J. Phys. Chem. B **117**, 9956 (2013).
[48]D. W. Marquardt, J. Soc. Ind. Appl. Math. **11**, 431 (1963).
[49]E. V. Ivash and D. M. Denninson, J. Chem. Phys. **21**, 1804 (1953).
[50]N. Sieffert, M. Buhl, M.-P. Gaigeot, and C. A. Morrison, J. Chem. Theory Comput. **9**, 106 (2013).
[51]I. Cibulka and M. Zikova, J. Chem. Eng. Data **39**, 876 (1994).
[52]D. Frenkel and B. Smit, *Understanding Molecular Simulation* (Academic Press, London, 2002).
[53]C. Vega, J. L. F. Abascal, and I. Nezbeda, J. Chem. Phys. **125**, 034503 (2006).
[54]R. C. Weast, *Handbook of Chemistry and Physics* (CRC, Boca Raton, 1986).
[55]C. A. Cerdeirina, C. A. Tovar, D. Gonzalez-Salgado, E. Carballo, and L. Romani, Phys. Chem. Chem. Phys. **3**, 5230 (2001).
[56]M. Lagache, P. Ungerer, A. Boutin, and A. H. Fuchs, Phys. Chem. Chem. Phys. **3**, 4333 (2001).
[57]M. Neumann, J. Chem. Phys. **50**, 841 (1983).

[58]C. Vega, Mol. Phys. **113**, 1145 (2015).
[59]C. Vega and E. de Miguel, J. Chem. Phys. **126**, 154707 (2007).
[60]M. A. Gonzalez and J. L. F. Abascal, J. Chem. Phys. **132**, 096101 (2010).
[61]D. Laage and W. H. Thompson, J. Chem. Phys. **136**, 044513 (2012).
[62]A. C. Fogarty, E. Duboue-Dijon, D. Laage, and W. H. Thompson, J. Chem. Phys. **141**, 18C523 (2014).
[63]D. V. der Spoel, E. Lindahl, B. Hess, G. Groenhof, A. E. Mark, and H. J. C. Berendsen, J. Comput. Chem. **26**, 1701 (2005).
[64]S. Yashonath and C. N. R. Rao, Mol. Phys. **54**, 245 (1985).
[65]M. Parrinello and A. Rahman, J. Appl. Phys. **52**, 7182 (1981).
[66]U. Essmann, L. Perera, M. L. Berkowitz, T. Darden, H. Lee, and L. G. Pedersen, J. Chem. Phys. **103**, 8577 (1995).
[67]S. Nosé, Mol. Phys. **52**, 255 (1984).
[68]W. G. Hoover, Phys. Rev. A **31** (1985).
[69]S. Nosé and M. L. Klein, Mol. Phys. **50**, 1055 (1983).
[70]J. L. F. Abascal and C. Vega, Phys. Rev. Lett. **98**, 237801 (2007).
[71]See supplementary material at http://dx.doi.org/10.1063/1.4958320 for tables with simulation data involved in the calculus of the solid-liquid equilibria of methanol OPLS/2016 and the worksheet for the computation of the scores of methanol models.
[72]M. Kettler, I. Nezbeda, A. A. Chialvo, and P. T. Cummings, J. Phys. Chem. B **106**, 7537 (2002).
[73]R. Goodwin, J. Phys. Chem. Ref. Data **16**, 799 (1987).
[74]J. Riddick, W. B. Bunger, and T. Sakano, *Organic Solvents. Physical Properties and Methods of Purification* (Wiley, New York, 1986).
[75]S. S. Chen, R. C. Wilhoit, and J. Zwolinski, J. Phys. Chem. Ref. Data **6**, 105 (1977).
[76]C. Vega, M. M. Conde, C. McBride, J. L. F. Abascal, E. G. Noya, L. M. Sese, and R. Ramirez, J. Chem. Phys. **12**, 046101 (2010).
[77]P. S. Albright and L. J. Gosting, J. Am. Chem. Soc. **68**, 1061 (1946).
[78]G. Vazquez, E. Alvarez, and J. M. Navaza, J. Chem. Eng. Data **40**, 611 (1995).
[79]O. Suarez-Iglesias, I. Medina, M. de los Angeles Sanz, C. Pizarro, and J. L. Bueno, J. Chem. Eng. Data **60**, 2757 (2015).
[80]H. W. Xiang, A. Laesecke, and M. L. Huber, J. Phys. Chem. Ref. Data **35**, 1597 (2006).
[81]R. Ludvig, C. Rusbuldt, P. Bopp, and M. D. Zeidler, Z. Natrusforsch. A **50**, 211 (1995).
[82]M. J. Gillan, D. Alfe, and A. Michaelides, J. Chem. Phys. **144**, 130901 (2016).
[83]E. Sanz, C. Vega, J. R. Espinosa, R. Caballero-Bernal, J. L. F. Abascal, and C. Valeriani, J. Am. Chem. Soc. **135**, 15008 (2013).
[84]J. R. Espinosa, E. Sanz, C. Valeriani, and C. Vega, J. Chem. Phys. **141**, 18C529 (2014).